Supplementary Figure Legends

Figure S1

Flowcytometry-based purity analysis of peritoneal macrophage culture.

Thioglycollate elicited peritoneal cells were incubated in culture dish for 2 hours in DMEM supplemented with 10% FBS and antibiotic. After washing of non-adherent cells, adherent macrophages were scraped from dish with rubber policeman and subjected to FITC-labeled CD115 antibody staining. A total of 50,000 or more cells were analyzed on a BD FACSCalibur flow cytometer and CD115 positive cells were recorded as macrophages. Histogram shown is representative of 3 different samples.

Figure S2

Time course of KLF4 gene expression.

Changes in KLF4 mRNA expression levels after treatment with LPS (50ng/ml), IFNγ (5ng/ml), IL4 (10ng/ml), IL13 (10ng/ml) and IL10 (10ng/ml) in (**A**) peritoneal macrophages (PM) and (**B**) bone marrow derived macrophages (BMDM). (**C**) Treatment of peritoneal macrophages with low dose of LPS (10ng/ml). n=3 for each time point. Data presented as mean ± SEM. *$p<0.05$, Student's t test with Bonferroni correction.

Figure S3

Characterization of myeloid-specific KLF4-deficient mice.

(**A**) Genotyping analysis of $LysM^{cre/cre}$ (Mye-WT) and $LysM^{cre/cre}$:$KLF4^{flox/flox}$ (Mye-KO) mice. (**B-D**) Deletion of KLF4 in Mye-KO macrophages as assessed by qPCR (**B** and **C**) and Western blot (**D**). n=3 in each group for qPCR. (**E**) Leukocytes cell populations are comparable in Mye-WT and Mye-KO mice as assayed by CBC (n=25 per genotype). (**F**) Monocyte population distribution ($Ly6C^{hi}$ vs. $Ly6C^{lo}$) is similar in Mye-WT and Mye-KO mice as analyzed by flow cytometry**.** Leukocytes were stained with fluorescent anti-CD115-RBE (MCA1898PET, AbDserotec), anti-CD11b-PerCP-Cy5.5 (550993, BD), and anti-Ly6C-FITC (553104, BD) antibodies, and cells gated from CD115+ were further analyzed for CD11b and Ly6C expression. n=3 in each genotype. *p<0.05, Student's *t* test with Bonferroni correction. N.S.: not significant.

Figure S4

KLF4 is involved in the regulation of Arg1 and and PPARγ expression.

(**A**) KLF4 enhanced IL4-induced Arg-1 expression. (**B**) KLF4 and Stat6 synergistically activate PPARγ promoter in RAW264.7 cells. n=3 in each group. (**C**) Requirement of KLF binding sites for optimal Arg-1 promoter activity. Schematic diagram of the IL4-responsive enhancer region of the mouse Arg-1 gene showing pertinent transcription factor binding sites. WT: ~4kb wild type mouse arg-1 promoter; ΔKLF**#**1: arg-1 promoter with 5' KLF-binding site (KLF#1) mutated; ΔKLF**#**2: arg-1 promoter with 3' KLF-binding site (KLF#2) mutated; ΔKLF**#**1&2: arg-1 promoter with both KLF-binding sites (KLF#1 and KLF#2) mutated. n=3 in each group. (**D**) ChIP analysis demonstrates that binding of Stat6 to the Arg-1 promoter is not affected by KLF4 deficiency or overexpression. (**E**) IL4-induced Stat6 phosphorylation is similar in WT and KLF4-deficient BMDM. Western blots of total cell protein were assessed by antibodies against total or phosphorylated Stat6. *p<0.05, Student's *t* test with Bonferroni correction.

Figure S5

Deficiency of KLF4 in macrophages enhanced LPS-induced M1 gene expression.

LPS induced enhanced secretion of MCP-1 (**A**) and TNFα (**B**) in Mye-KO macrophages medium. Cytokine levels were determined by ELISA. n=3 in each group. *p<0.05, Student's *t* test.

Figure S6

LPS-induced pro-inflammation genes expression and NO production in WT and Stat6-null macrophages.

(**A**-**E**) qPCR analysis of pro-inflammation genes in control and LPS-treated peritoneal macrophages from WT and Stat6-null mice. n=3 in each group. (**F**) LPS-induced NO production in WT and Stat6-null macrophages as assayed by nitrate concentration in conditioned medium. n=3 for each data point. *p<0.05, Student's *t* test. N.S.: not significant.

Figure S7

Non-specific PCR for Cox-2 promoter using non-targeting primers.

PCR was performed with sense-primers: ATTCAAGCAGCAGAAGAGGGCAG and antisense-primer: CTGGGATGCCAGAGCACACTG.

Figure S8

IL4-pretreatment inhibits subsequent LPS-mediated induction of M1 genes in Mye-WT macrophages but not in Mye-KO macrophages. n=3 for each data point. *p<0.05, Student's *t* test with Bonferroni correction. N.S.: not significant.

Figure S9

KLF4 deficient macrophage exhibit enhanced bactericidal activity.

(**A** and **B**) KLF4-deficient macrophages exhibit enhanced bactericidal activity against *S. aureus* ex vivo. n=3 in each genotype. (**C**) NOX1 expression is augmented in KLF4 deficient macrophages after incubation with S. aureus. n=3 for each data point. *p<0.05, Student's *t* test with Bonferroni correction.

Figure S10

Myeloid KLF4 deficiency does not affect bacterial uptake ability of macrophages.

WT and KLF4-deficient macrophages take up similar amounts of K-12 E. coli bio-particles as revealed by fluorescent microscopy (**A**) and flow cytometry assay (**B**). Image shown are representative from 3 sets of samples.

Figure S11

Infiltration of macrophages in skin wound and in vitro migration assay of macrophages.

(**A**) No difference is observed in the numbers of infiltrated macrophages in skin wound between Mye-WT and Mye-KO mice as analyzed by immunohistochemistry. n=3 in each group. (**B**) No difference in MCP-1 (CCL2) induced migration between WT and KLF4-deficient macrophages as assessed by Boyden chamber assay. n=3 in each group. N.S.: not significant as determined by Student's *t* test.

Figure S12

KLF2 and KLF4 expression levels in different human adipose tissues and KLF4 expression in different cells of adipose tissues.

(**A**) Compared with subcutaneous fat, visceral fat has lower expression of KLF4 but not of KLF2. Data represented were from 24 OB patient samples. (**B**) KLF4 is predominantly expressed by macrophages in adipose tissue. Cells were isolated from 4 OB patients. *p<0.05, Kruskal–Wallis test.

Figure S13

Metabolic changes in Mye-WT and Mye-KO mice after HFD.

(**A**) Representative MRI images of body composition. (**B**) Mye-KO mice demonstrate higher level of total triglycerides in plasma (n=6 per genotype). (**C** and **D**) HDL and LDL levels in plasma remain similar between Mye-WT and Mye-KO after HFD. *p<0.05, Student's *t* test. N.S.: not significant.

Figure S14

Food intakes and energy expenditure in Mye-WT and Mye-KO mice.

(**A**) Food intake during a 24h period. (**B**) Respiration and heat production analysis. n=5 in each group. *p<0.05, Student's *t* test with Bonferroni correction. N.S.: not significant.

Figure S15

Impaired insulin signaling in HFD-fed Mye-KO mice.

(**A**) Serum insulin levels in Mye-WT and Mye-KO mice. n=6 in each group. (**B**) Baseline glucose tolerance test in Mye-WT and Mye-KO mice. n=6 in each group. (**C**) Impaired insulin signaling in Mye-KO mice after 12-week HFD as determined by phosphorylation of Akt. One animal in Saline group and two animals in Insulin-stimulated group were shown for each genotype.*p<0.05, Student's *t* test.

Figure S16

Myeloid deficiency of KLF4 results in alteration of expression of select metabolic and inflammatory genes in HFD-fed mice.

(**A**) Quadriceps muscle. (**B**) Liver tissue. n=6 per genotype. p value by Student's *t* test.

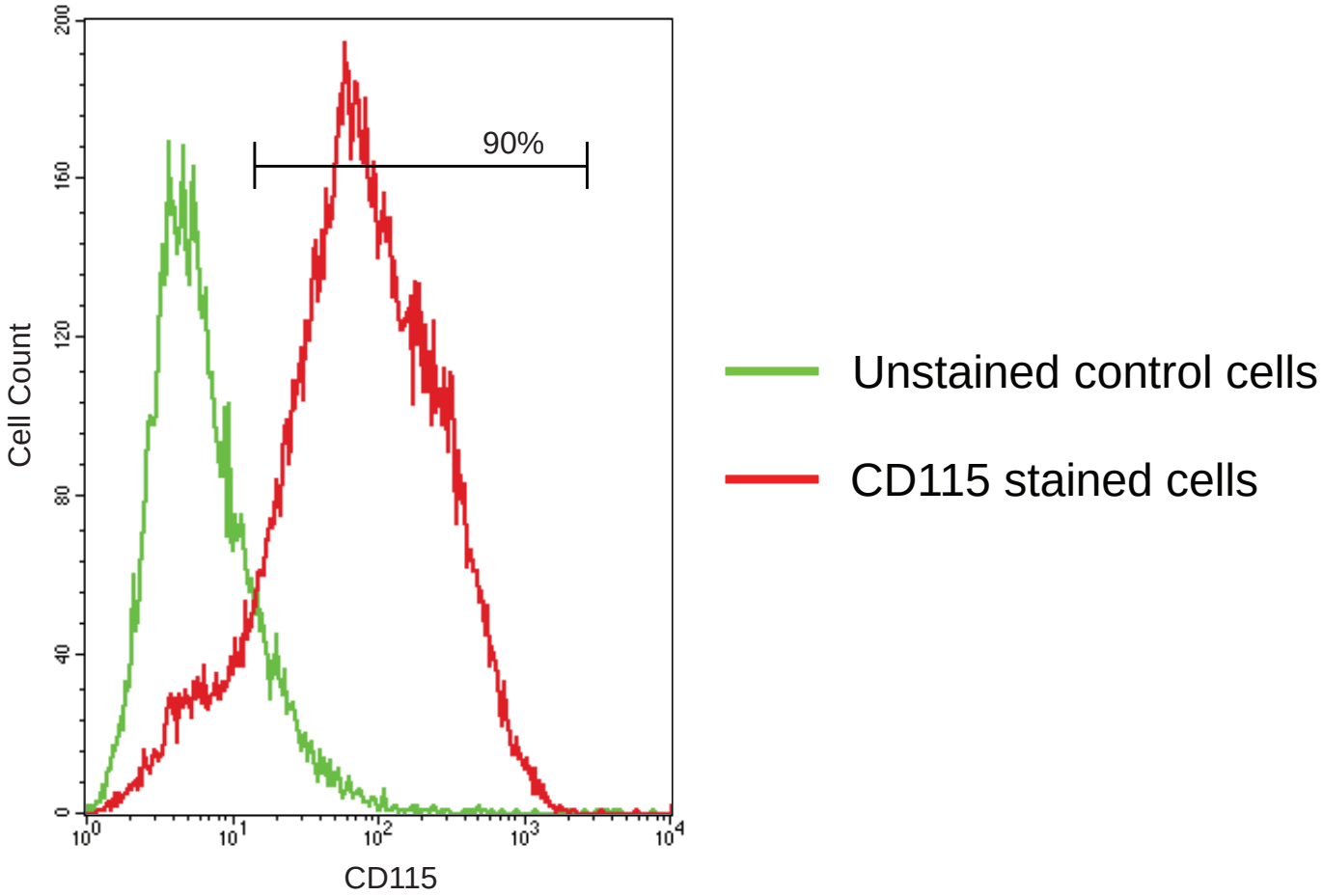
200
160
120
80
40
0
Cell Count
90%
10^0
10^1
10^2
10^3
10^4
CD115
Unstained control cells
CD115 stained cells

Figure S1

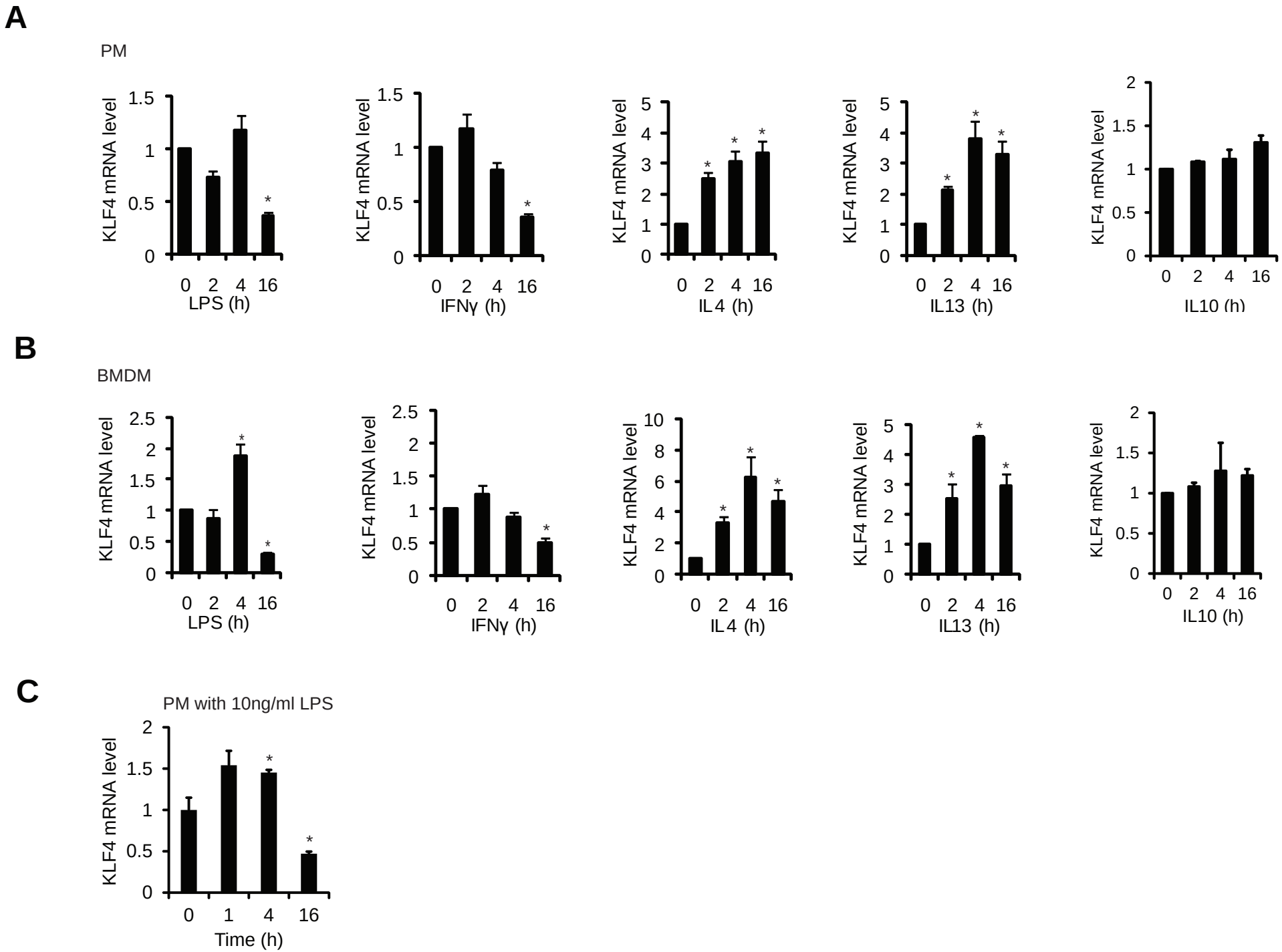
A
PM
KLF4 mRNA level
LPS (h)
IFNγ (h)
IL4 (h)
IL13 (h)
IL10 (h)
B
BMDM
KLF4 mRNA level
LPS (h)
IFNγ (h)
IL4 (h)
IL13 (h)
IL10 (h)
C
PM with 10ng/ml LPS
KLF4 mRNA level
Time (h)

Figure S2

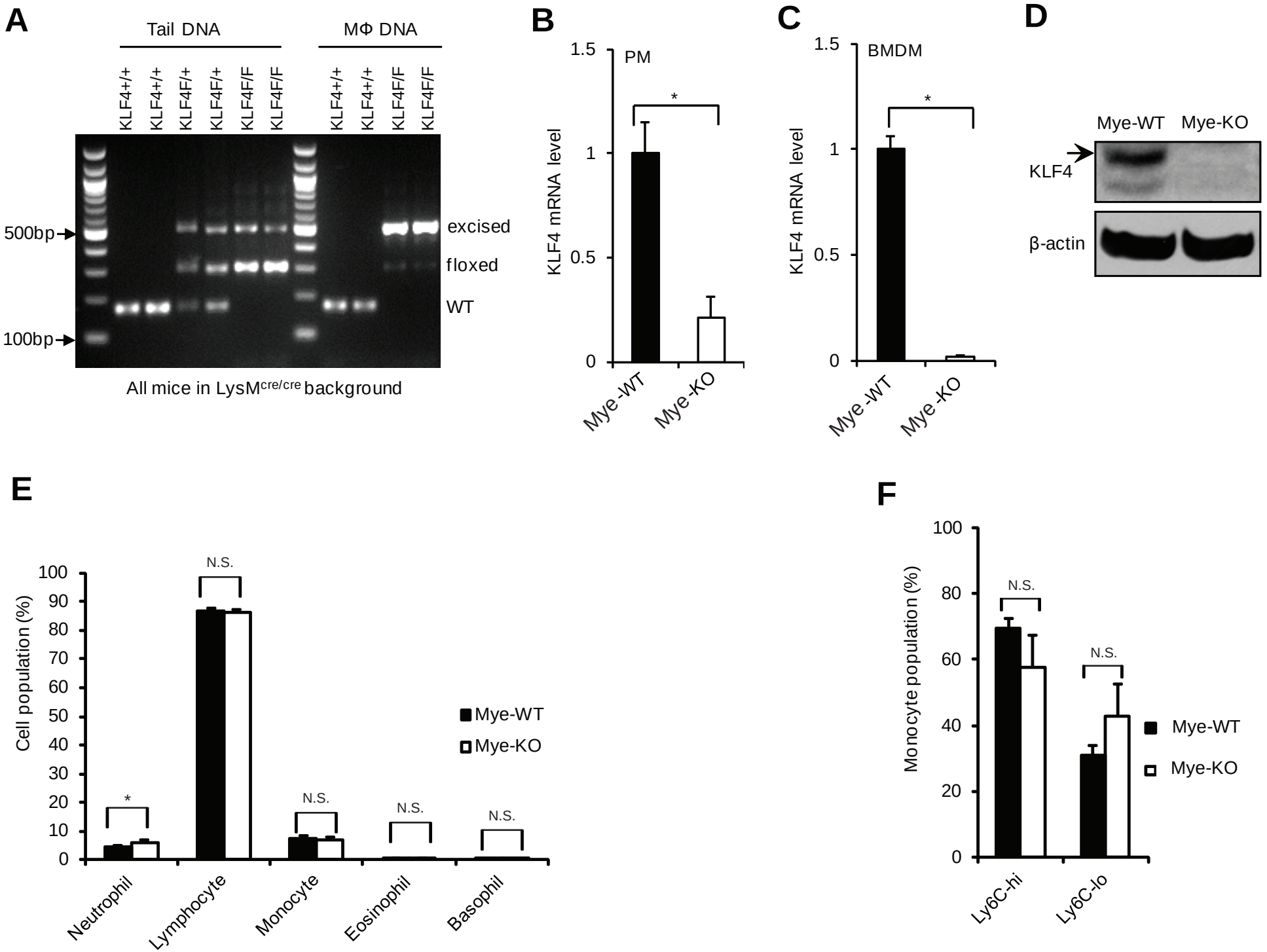
A
Tail DNA
MΦ DNA
KLF4+/+
KLF4+/+
KLF4F/+
KLF4F/+
KLF4F/F
KLF4F/F
KLF4+/+
KLF4+/+
KLF4F/F
KLF4F/F
500bp
100bp
excised
floxed
WT
All mice in LysM cre/cre background
B
PM
KLF4 mRNA level
1.5
1
0.5
0
*
Mye-WT
Mye-KO
C
BMDM
KLF4 mRNA level
1.5
1
0.5
0
*
Mye-WT
Mye-KO
D
Mye-WT
Mye-KO
KLF4
β-actin
E
Cell population (%)
100
90
80
70
60
50
40
30
20
10
0
N.S.
*
N.S.
N.S.
N.S.
Mye-WT
Mye-KO
Neutrophil
Lymphocyte
Monocyte
Eosinophil
Basophil
F
Monocyte population (%)
100
80
60
40
20
0
N.S.
N.S.
Mye-WT
Mye-KO
Ly6C-hi
Ly6C-lo

Figure S3

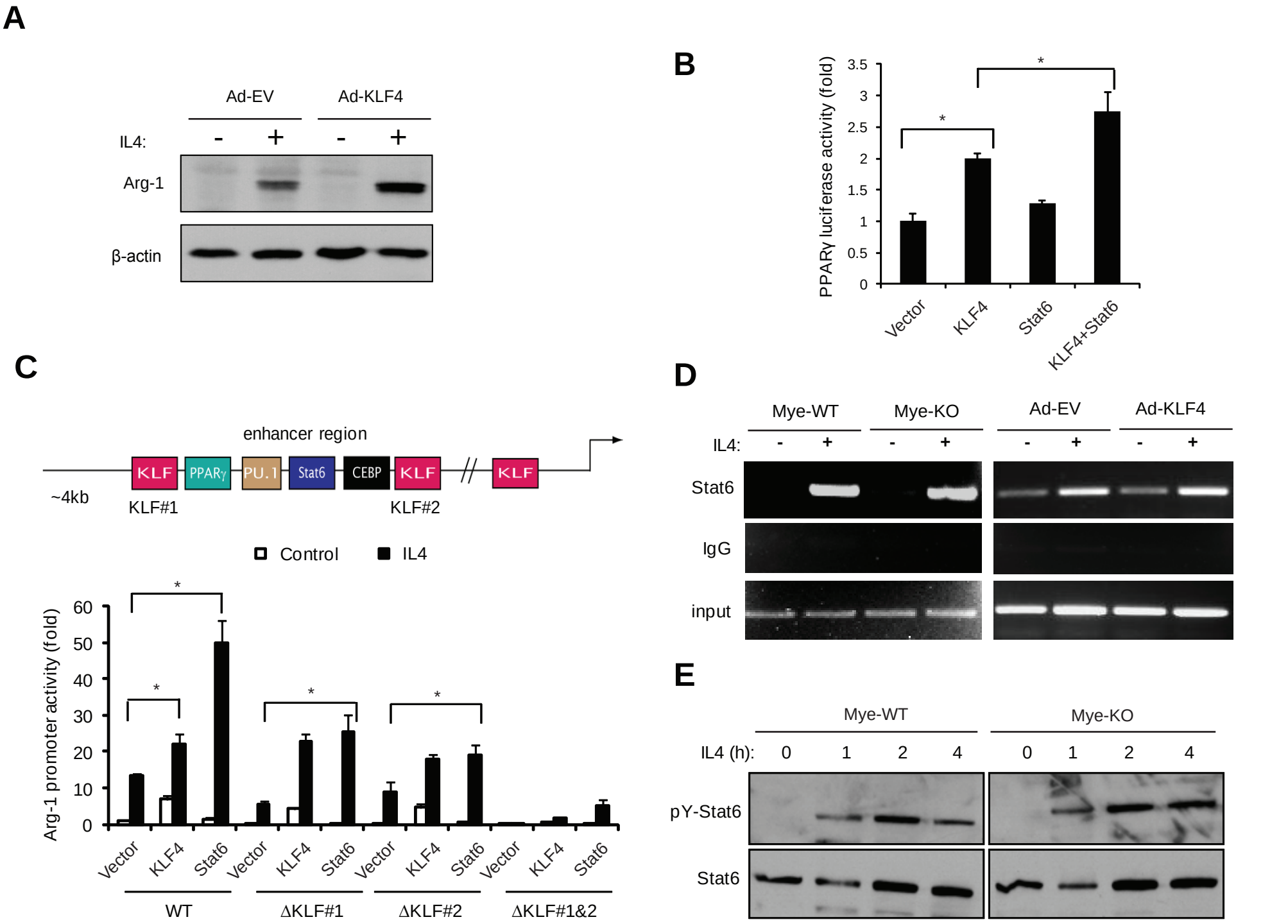
A
Ad-EV
Ad-KLF4
IL4:
- + - +
Arg-1
β-actin
B
PPARγ luciferase activity (fold)
3.5
3
2.5
2
1.5
1
0.5
0
*
*
Vector
KLF4
Stat6
KLF4+Stat6
C
enhancer region
KLF
PPARγ
PU.1
Stat6
CEBP
KLF
KLF
~4kb
KLF#1
KLF#2
Control
IL4
Arg-1 promoter activity (fold)
60
50
40
30
20
10
0
Vector
KLF4
Stat6
WT
ΔKLF#1
ΔKLF#2
ΔKLF#1&2
D
Mye-WT
Mye-KO
Ad-EV
Ad-KLF4
IL4:
Stat6
IgG
input
E
Mye-WT
Mye-KO
IL4 (h):
0 1 2 4 0 1 2 4
pY-Stat6
Stat6

Figure S4

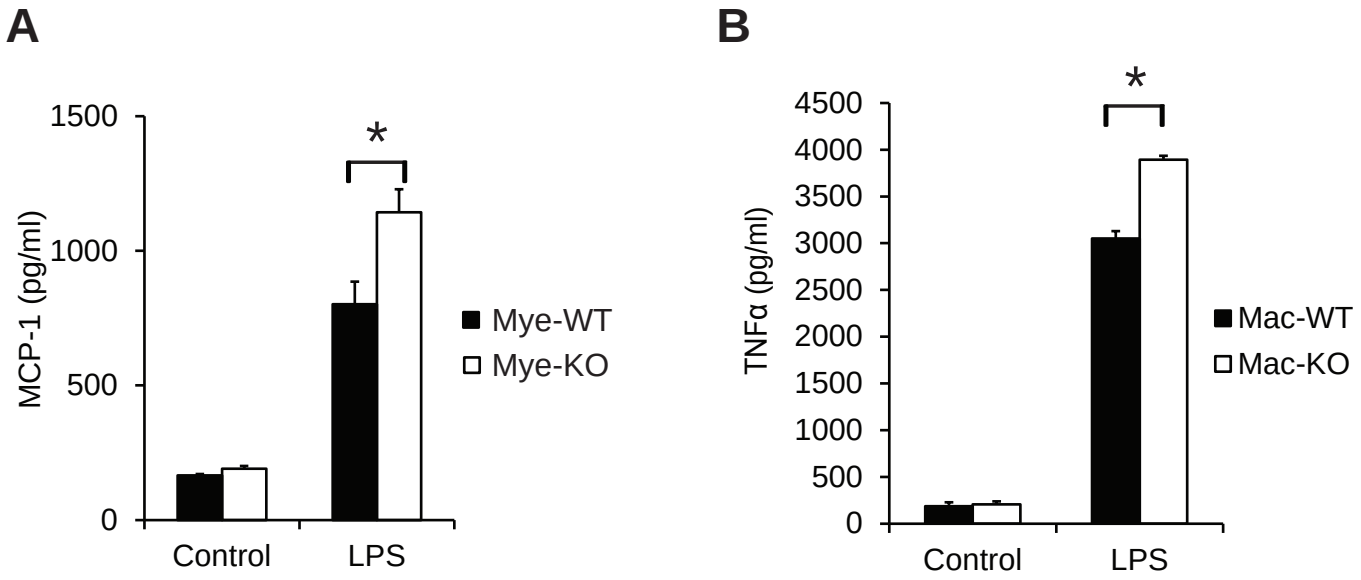
A
1500
1000
500
0
MCP-1 (pg/ml)
*
Control
LPS
Mye-WT
Mye-KO
B
4500
4000
3500
3000
2500
2000
1500
1000
500
0
TNFα (pg/ml)
*
Control
LPS
Mac-WT
Mac-KO

Figure S5

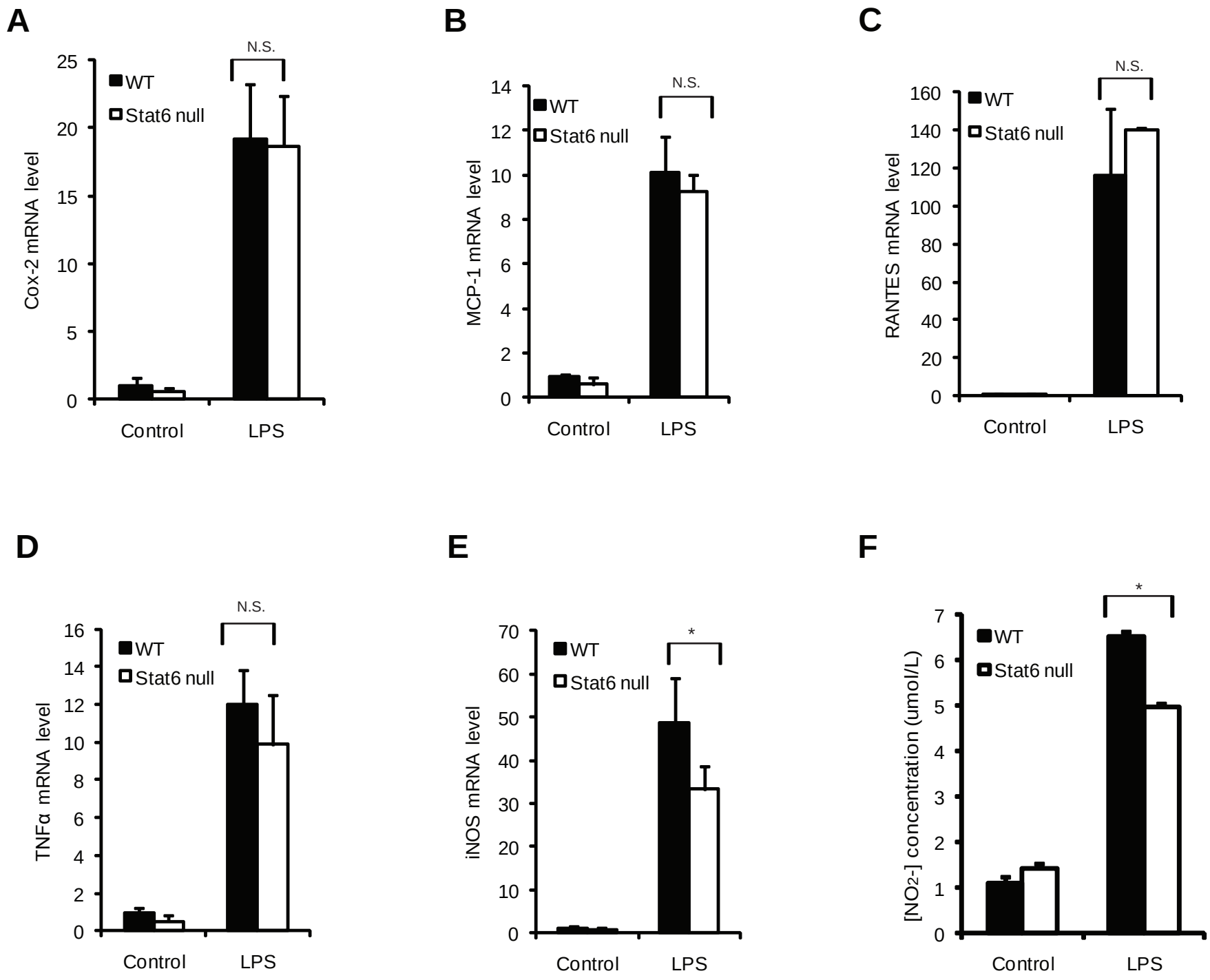
A
N.S.
WT
Stat6 null
Cox-2 mRNA level
25
20
15
10
5
0
Control
LPS
B
N.S.
WT
Stat6 null
MCP-1 mRNA level
14
12
10
8
6
4
2
0
Control
LPS
C
N.S.
WT
Stat6 null
RANTES mRNA level
160
140
120
100
80
60
40
20
0
Control
LPS
D
N.S.
WT
Stat6 null
TNFα mRNA level
16
14
12
10
8
6
4
2
0
Control
LPS
E
*
WT
Stat6 null
iNOS mRNA level
70
60
50
40
30
20
10
0
Control
LPS
F
*
WT
Stat6 null
[NO2-] concentration (umol/L)
7
6
5
4
3
2
1
0
Control
LPS

Figure S6

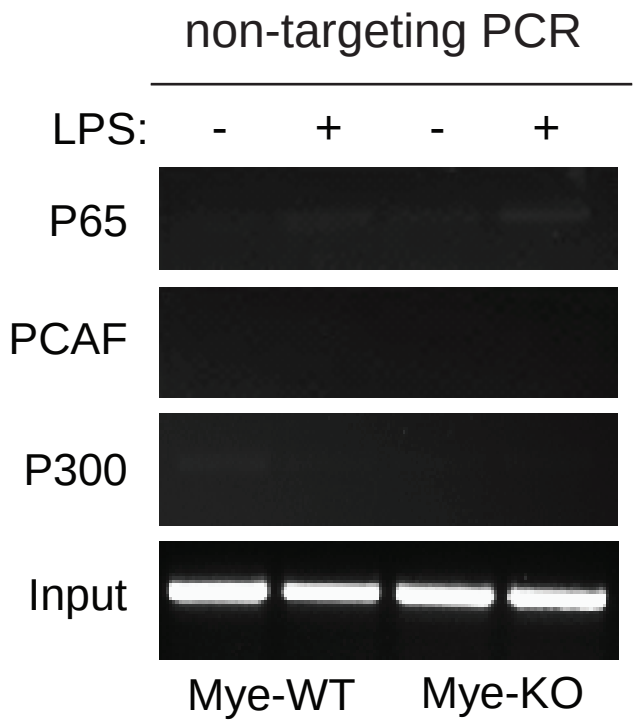

Figure S7

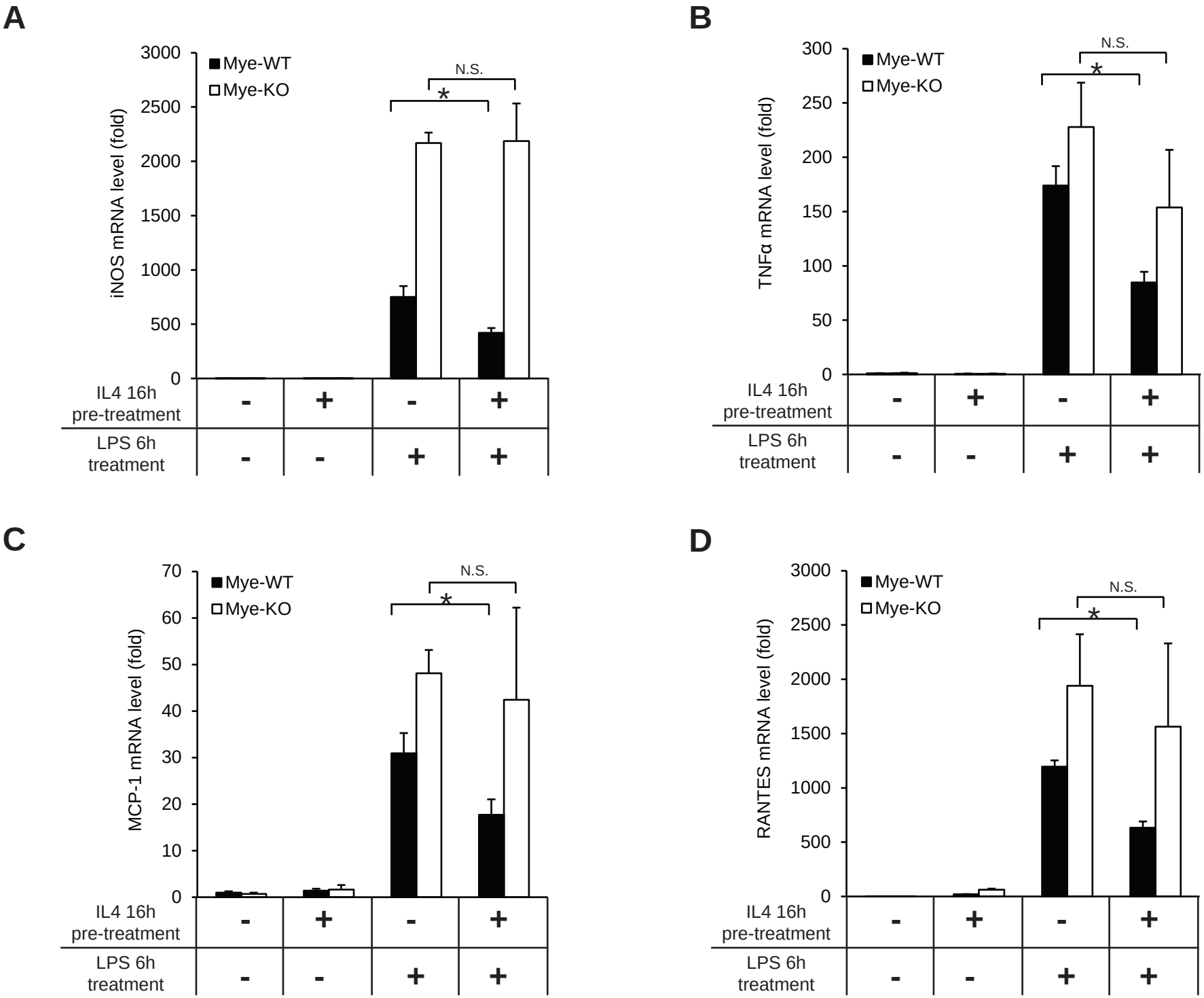
A
iNOS mRNA level (fold)
3000
2500
2000
1500
1000
500
0
Mye-WT
Mye-KO
N.S.
*
IL4 16h pre-treatment
LPS 6h treatment
- + - +
- - + +
B
TNFα mRNA level (fold)
300
250
200
150
100
50
0
Mye-WT
Mye-KO
N.S.
*
IL4 16h pre-treatment
LPS 6h treatment
- + - +
- - + +
C
MCP-1 mRNA level (fold)
70
60
50
40
30
20
10
0
Mye-WT
Mye-KO
N.S.
*
IL4 16h pre-treatment
LPS 6h treatment
- + - +
- - + +
D
RANTES mRNA level (fold)
3000
2500
2000
1500
1000
500
0
Mye-WT
Mye-KO
N.S.
*
IL4 16h pre-treatment
LPS 6h treatment
- + - +
- - + +

Figure S8

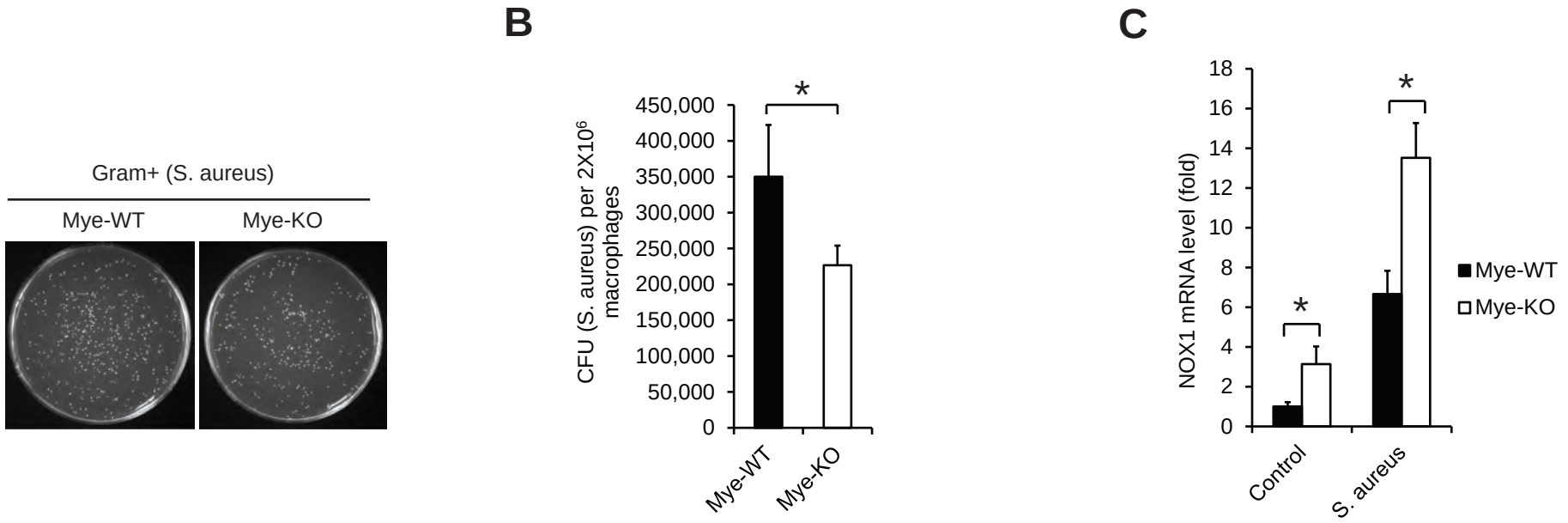
A
Gram+ (S. aureus)
Mye-WT
Mye-KO
B
CFU (S. aureus) per 2X10^6 macrophages
450,000
400,000
350,000
300,000
250,000
200,000
150,000
100,000
50,000
0
*
Mye-WT
Mye-KO
C
NOX1 mRNA level (fold)
18
16
14
12
10
8
6
4
2
0
*
*
Mye-WT
Mye-KO
Control
S. aureus

Figure S9

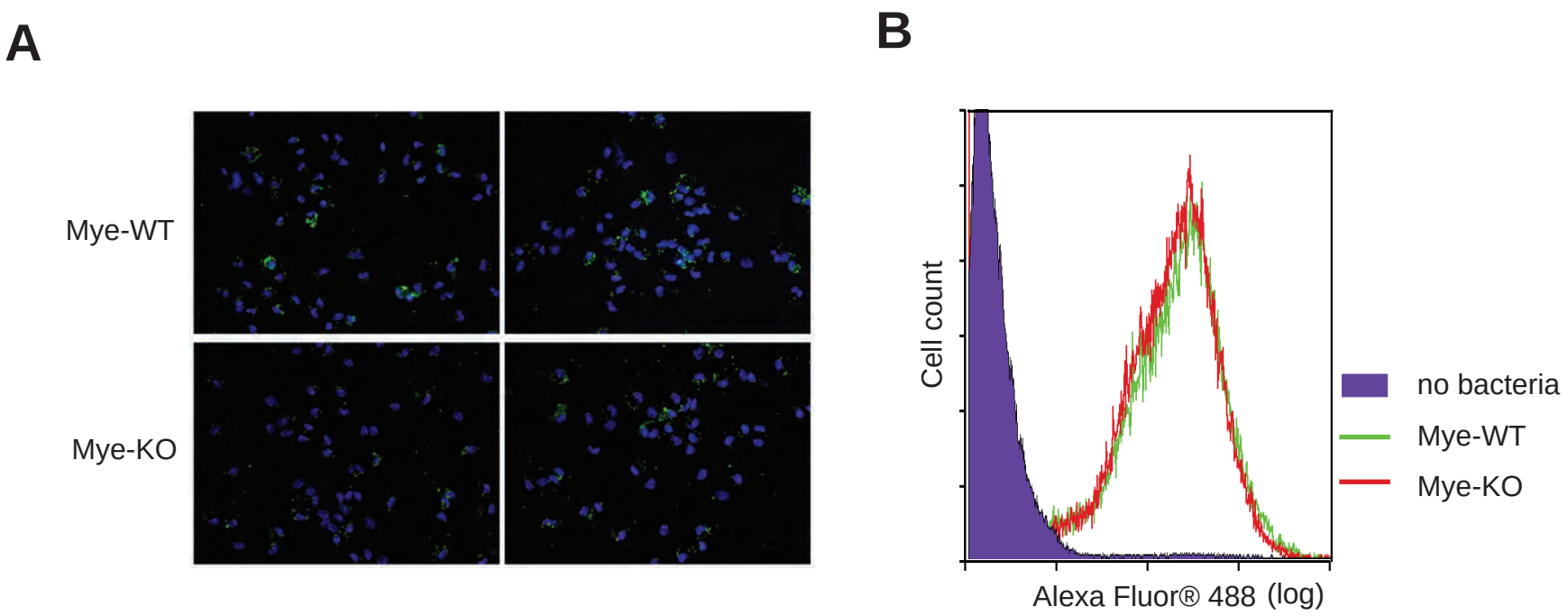
A
Mye-WT
Mye-KO
B
Cell count
Alexa Fluor® 488 (log)
no bacteria
Mye-WT
Mye-KO

Figure S10

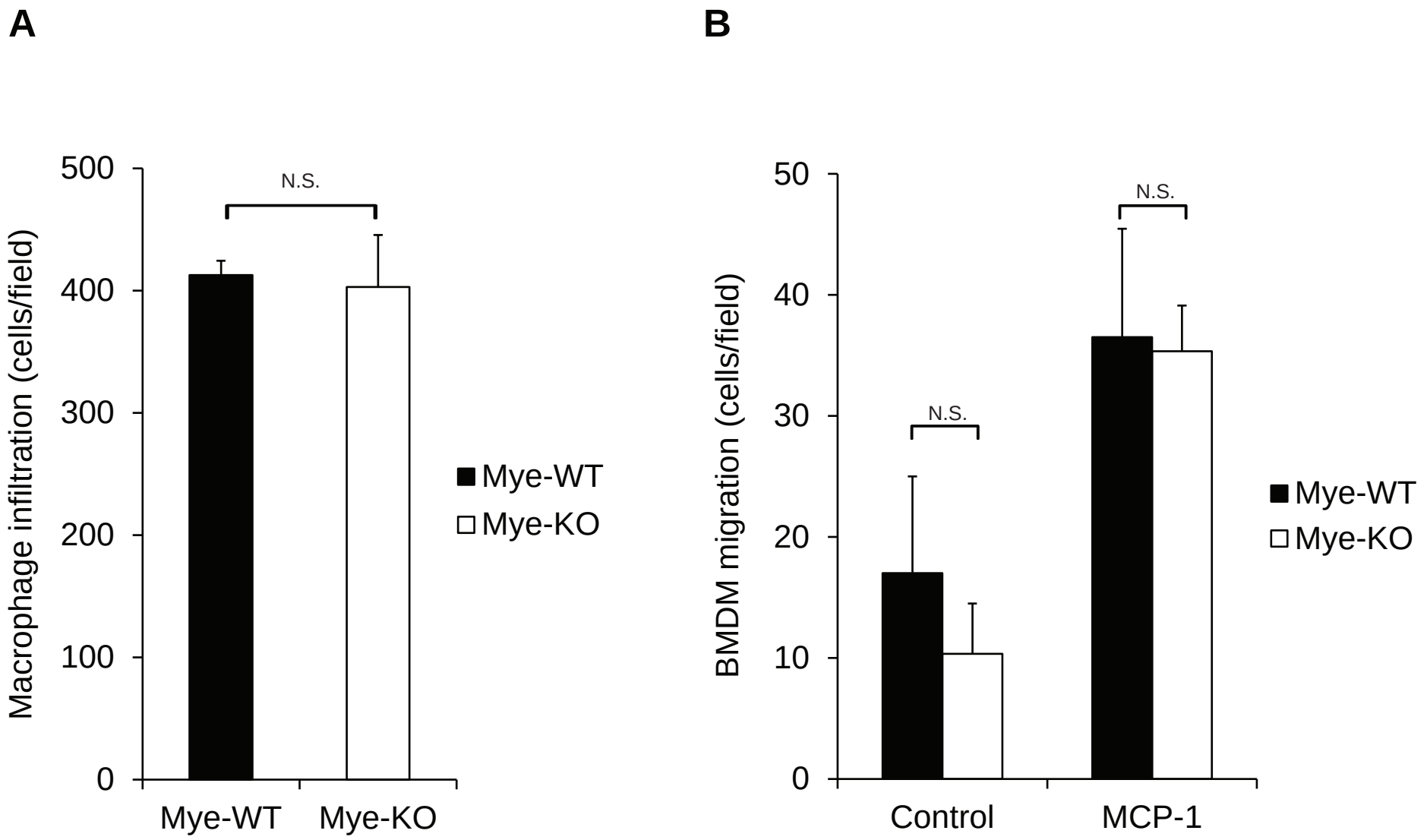
A
500
400
300
200
100
0
Macrophage infiltration (cells/field)
N.S.
Mye-WT
Mye-KO
Mye-WT
Mye-KO
B
50
40
30
20
10
0
BMDM migration (cells/field)
N.S.
N.S.
Mye-WT
Mye-KO
Control
MCP-1

Figure S11

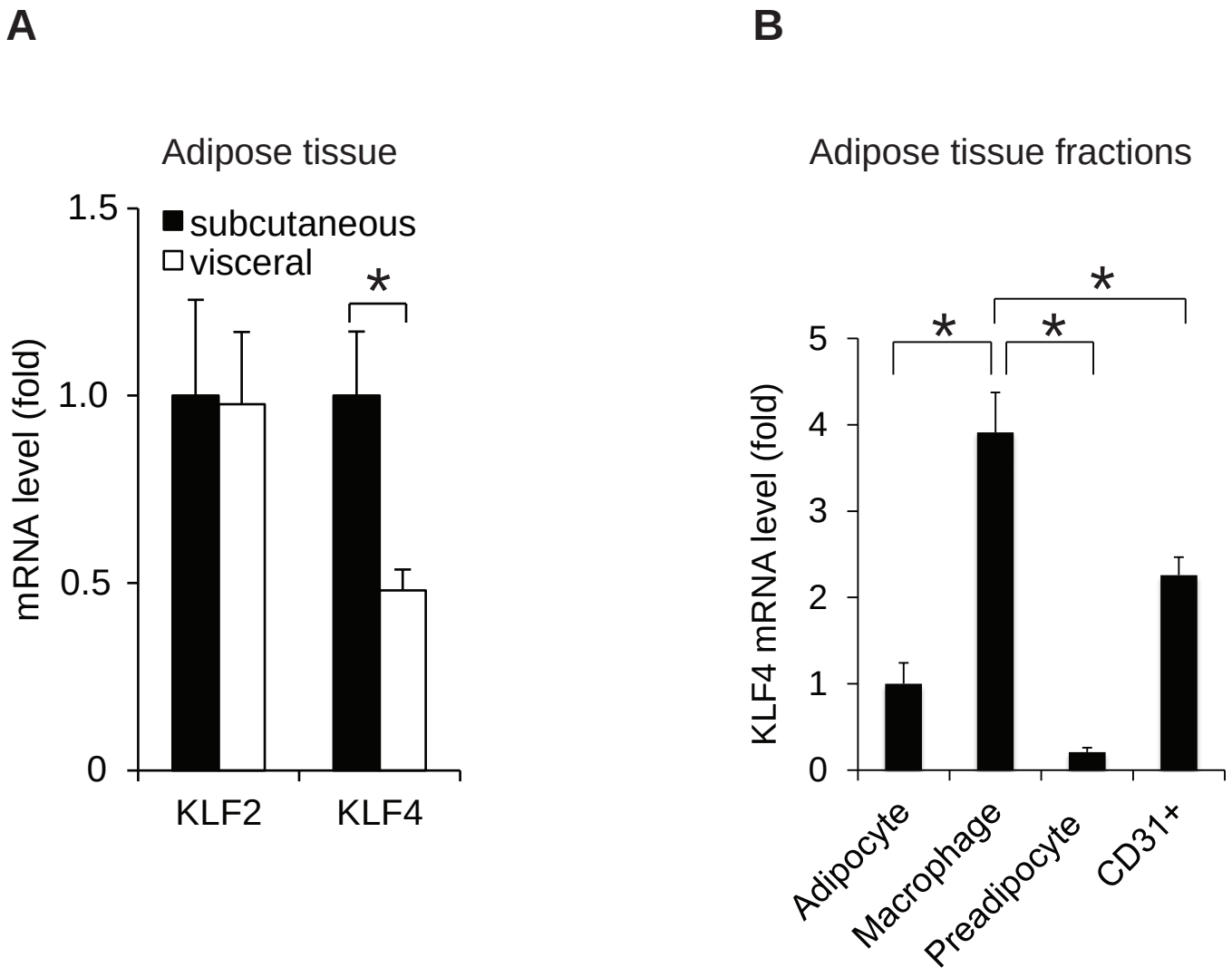
A
Adipose tissue
1.5
1.0
0.5
0
mRNA level (fold)
subcutaneous
visceral
*
KLF2
KLF4
B
Adipose tissue fractions
*
*
*
5
4
3
2
1
0
KLF4 mRNA level (fold)
Adipocyte
Macrophage
Preadipocyte
CD31+

Figure S12

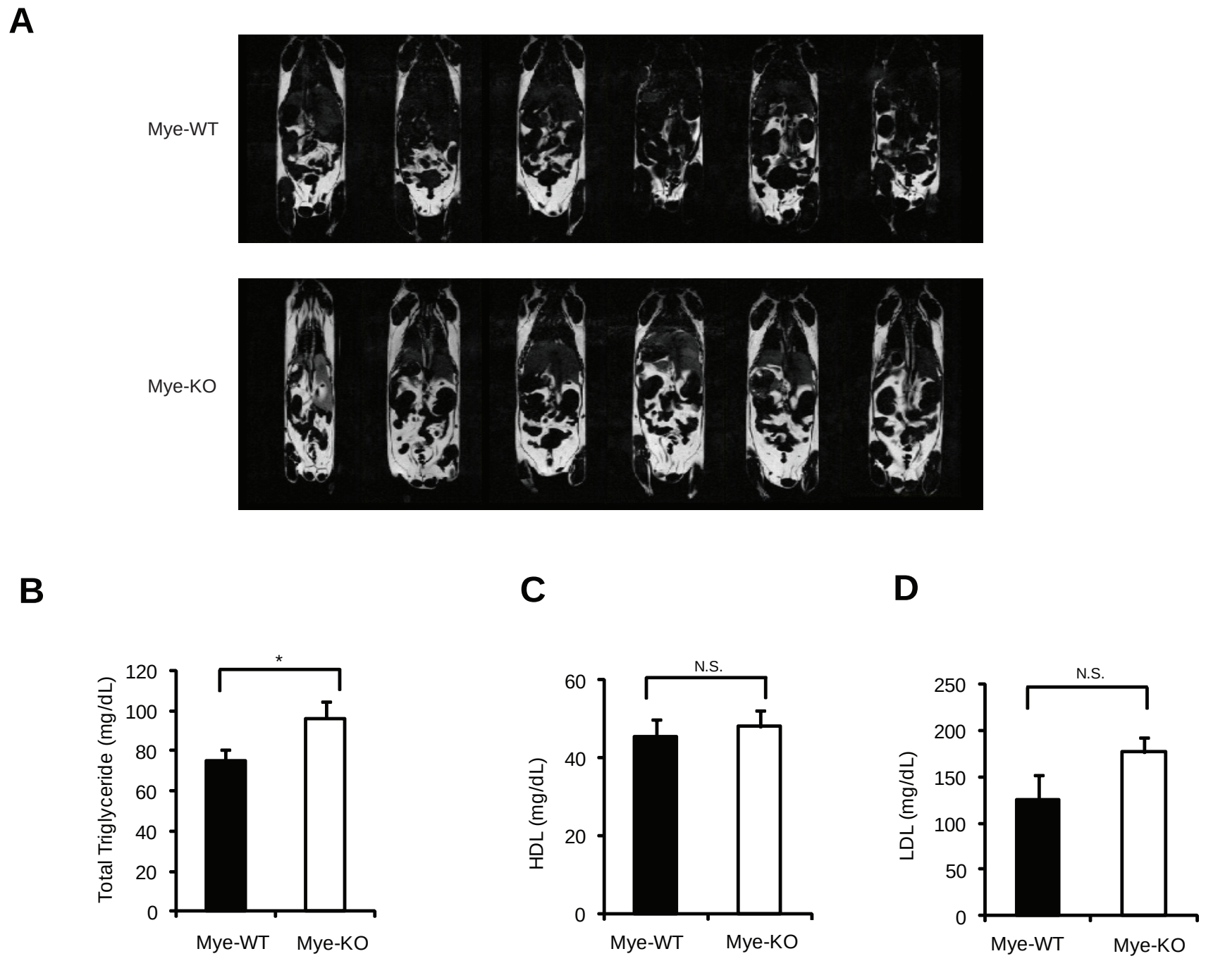
A
Mye-WT
Mye-KO
B
Total Triglyceride (mg/dL)
120
100
80
60
40
20
0
*
Mye-WT
Mye-KO
C
HDL (mg/dL)
60
40
20
0
N.S.
Mye-WT
Mye-KO
D
LDL (mg/dL)
250
200
150
100
50
0
N.S.
Mye-WT
Mye-KO

Figure S13

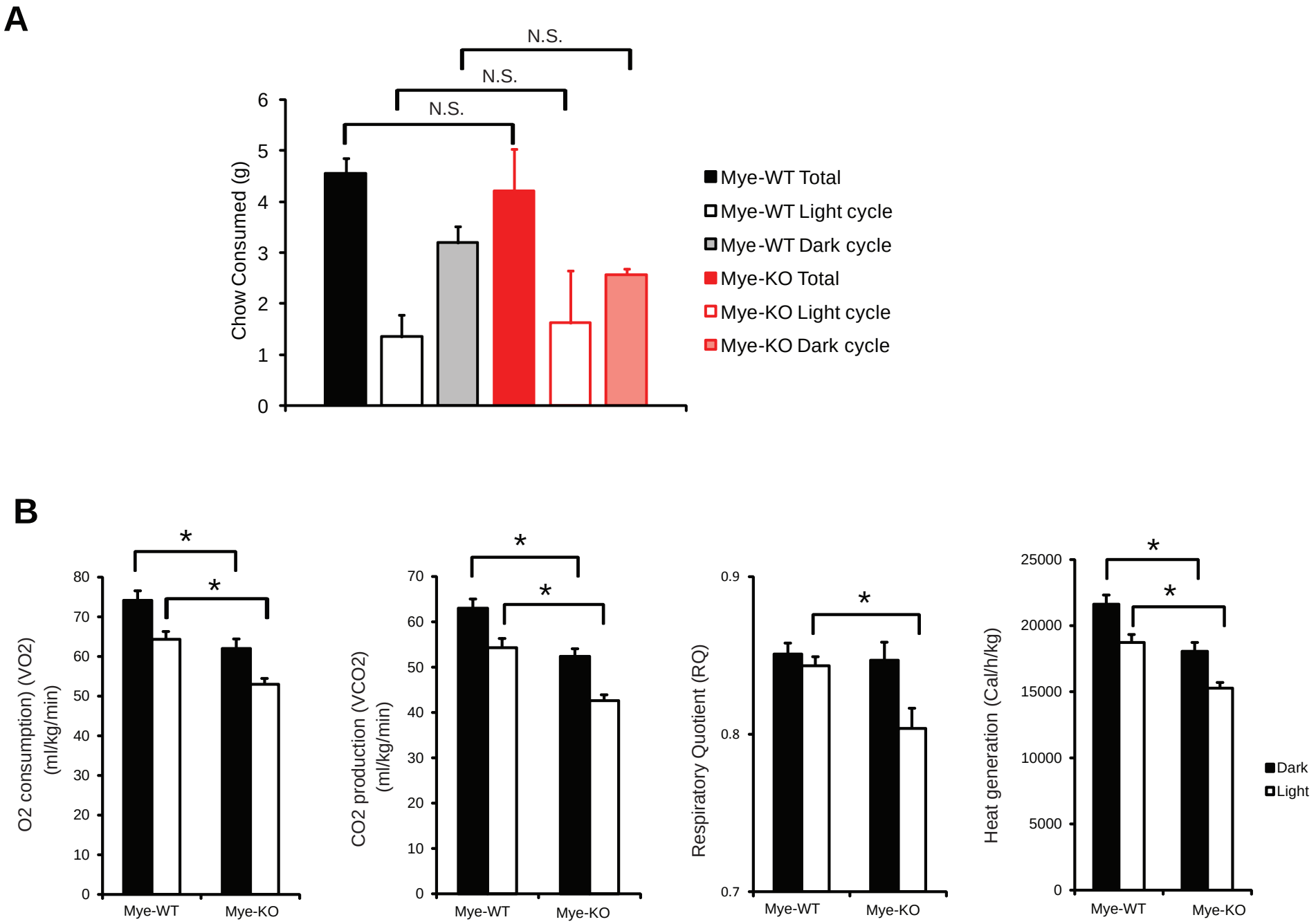
A
N.S.
N.S.
N.S.
Chow Consumed (g)
0
1
2
3
4
5
6
Mye-WT Total
Mye-WT Light cycle
Mye-WT Dark cycle
Mye-KO Total
Mye-KO Light cycle
Mye-KO Dark cycle
B
O2 consumption) (VO2) (ml/kg/min)
CO2 production (VCO2) (ml/kg/min)
Respiratory Quotient (RQ)
Heat generation (Cal/h/kg)
Mye-WT
Mye-KO
Dark
Light

Figure S14

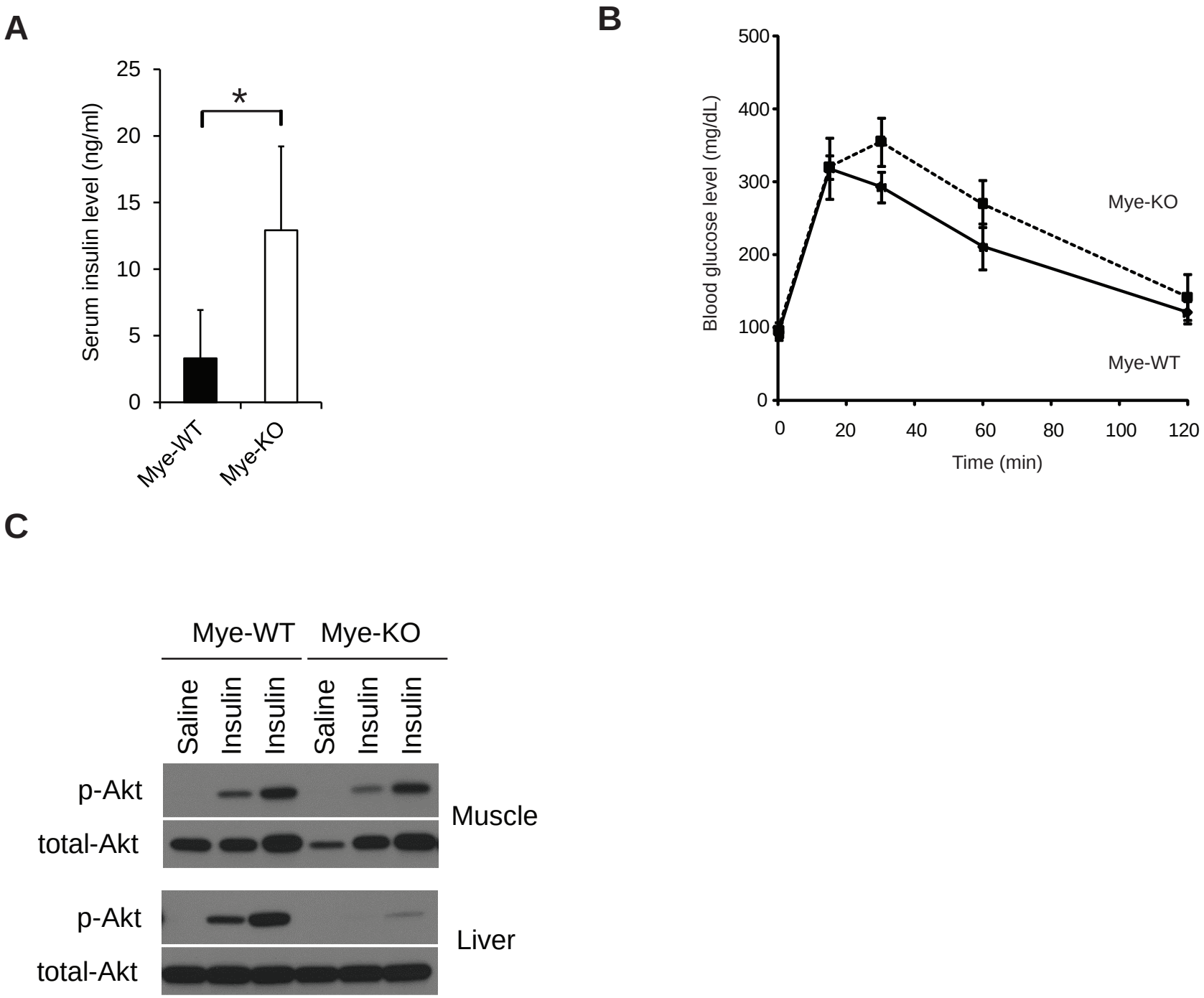
A
Serum insulin level (ng/ml)
25
20
15
10
5
0
*
Mye-WT
Mye-KO
B
Blood glucose level (mg/dL)
500
400
300
200
100
0
Mye-KO
Mye-WT
0
20
40
60
80
100
120
Time (min)
C
Mye-WT
Mye-KO
Saline
Insulin
Insulin
Saline
Insulin
Insulin
p-Akt
total-Akt
Muscle
p-Akt
total-Akt
Liver

Figure S15

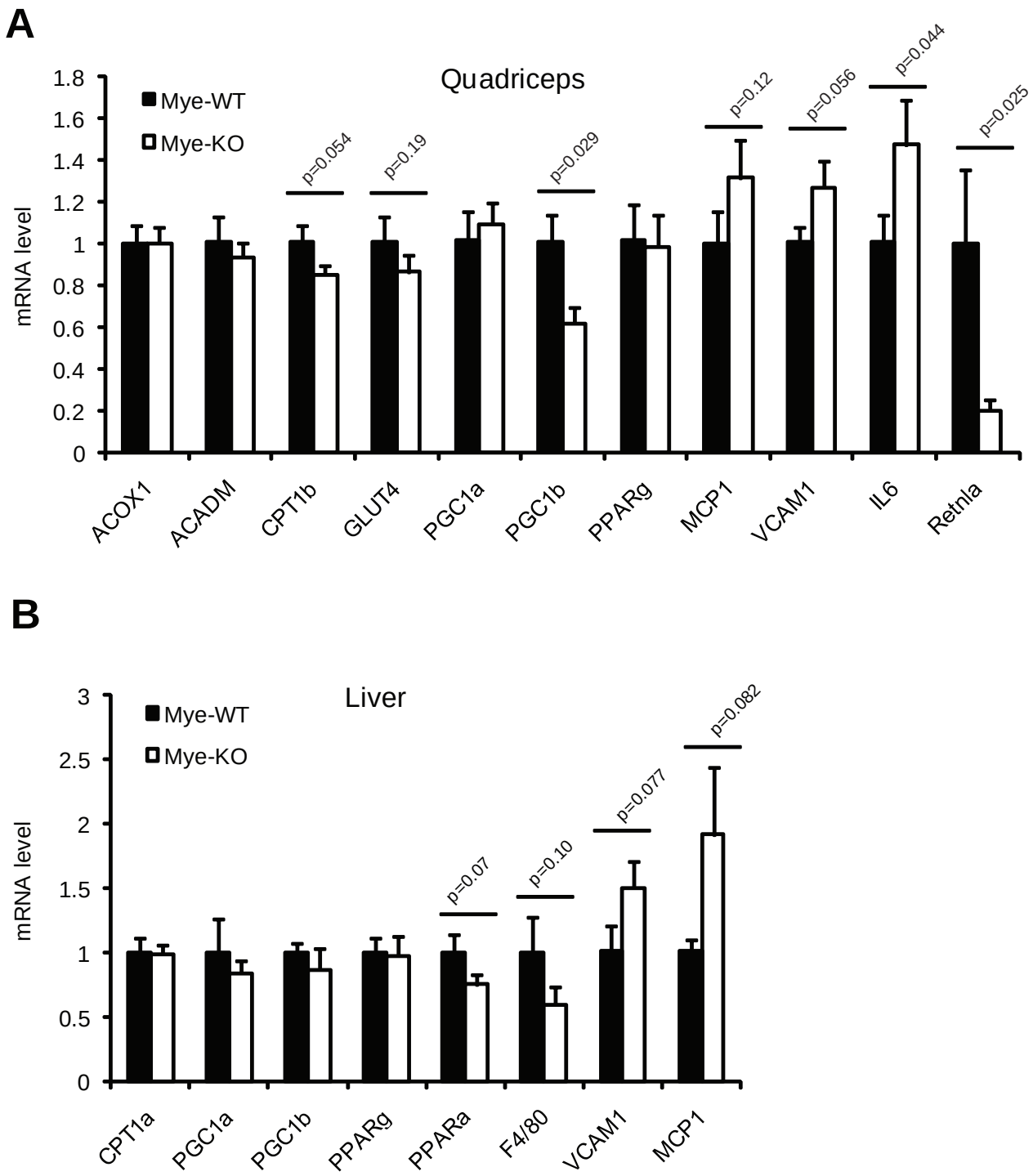
A
Quadriceps
Mye-WT
Mye-KO
mRNA level
1.8
1.6
1.4
1.2
1
0.8
0.6
0.4
0.2
0
p=0.054
p=0.19
p=0.029
p=0.12
p=0.056
p=0.044
p=0.025
ACOX1
ACADM
CPT1b
GLUT4
PGC1a
PGC1b
PPARg
MCP1
VCAM1
IL6
Retnla
B
Liver
Mye-WT
Mye-KO
mRNA level
3
2.5
2
1.5
1
0.5
0
p=0.07
p=0.10
p=0.077
p=0.082
CPT1a
PGC1a
PGC1b
PPARg
PPARa
F4/80
VCAM1
MCP1

Figure S16